

Quad-Port Miniaturized Ultra-Wideband MIMO Antenna with Metal Vias

Qingzhi Yang^{1, 2}, Kang Wang², and Yufa Sun^{2, *}

Abstract—A miniaturized four-port multiple-input multiple-output (MIMO) antenna for ultra-wideband (UWB) applications is presented. The proposed UWB MIMO antenna has a compact size of $34 \times 34 \text{ mm}^2$. Four antenna elements are placed orthogonally, and the element is connected to the feed line through metal vias in the substrate. These metal vias increase the bandwidth of the high frequency part of the antenna. A T-shaped slit, a rectangular slit, and a triangular chamfer are etched on the ground between two adjacent antenna elements. The working bandwidth of the antenna is 2.5–11.6 GHz, covering the entire UWB application band. The isolation between antenna elements is more than 18 dB within the operating bandwidth. Details of the design methodology and results are presented and discussed. Envelope correlation coefficient is computed, and it is within the acceptable limit, which validates the design concept for building a compact MIMO antenna system with good performance.

1. INTRODUCTION

Since its introduction to civilian use, UWB technology has attracted the attention of relevant personnel in the field of microwave communication due to its large information capacity, low energy consumption, and availability for positioning. Owing to these advantages, the UWB technology has been adopted widely in many applications such as short-range indoor communications, cognitive radio, sensing and imaging systems, radar, and target positioning [1, 2]. MIMO technology has attracted significant research attention for its well-known advantages such as reducing multipath fading and increasing transmission capacity. The antenna for MIMO system should be designed to ensure that the isolation between the elements is greater than 15 dB [3–5]. The application of UWB technology to MIMO antennas for short-range communication is a hot topic at present [6, 7].

In order to increase the isolation between the antenna elements, several dual-port antennas for adding stubs on the ground plane are reported in [8–10]. The isolation between the elements of the antenna is increased due to a T-shaped ground stub [8], two F-shaped ground stubs [9], two L-shaped ground stubs [10], and a rectangular slit [11]. The mutual coupling between the antenna elements and the coupling of the ground branches cancel each other out. In addition, a filter structure is placed on the coplanar ground to reduce mutual coupling, which complicates the structure of the antenna. High isolation is obtained by using meander line [12] and electromagnetic band gap (EBG) structures [13]. The dual-port MIMO antennas cannot meet the demand for large channels in life, and more ports for MIMO antenna design are needed. The antenna with four elements [13–17] is reported with enhanced isolation by orienting elements orthogonal to each other. The miniaturization and wideband phenomena [14] are achieved by using Koch fractal at the edges of the octagonal monopole, and isolation enhancement is done by utilizing ground stubs [14, 16, 17]. The high isolation is achieved by placing decoupling resonators between elements on the top and bottom layers of the model [17]. In [18, 19], the distance

Received 6 February 2021, Accepted 2 April 2021, Scheduled 12 April 2021

* Corresponding author: Yufa Sun (yfsun_ahu@sina.com).

¹ Department of Intelligent Engineering, Bozhou Vocational and Technical College, Bozhou 236800, China. ² Key Lab. of Intelligent Computing & Signal Processing, Ministry of Education, Anhui University, Hefei 230601, China.

between the units was increased to improve the isolation. References [20, 21] use the method of placing the antenna perpendicular to the ground to achieve a better isolation effect, which makes the size of the antenna become very large. However, the above MIMO antennas are designed with very large sizes, and smaller size UWB-MIMO antennas with high isolation are required.

In this paper, a quad-port miniaturized UWB-MIMO antenna with high isolation is presented. The four elements are placed perpendicularly, which can reduce the coupling between the elements by using the polarization diversity feature. In addition, the element feedline is placed at the corner of the substrate so that the distance between the elements is large enough to perform the design of the ground branch. The nine periodically arranged metal vias are integrated into the substrate between the feedline and the patch, and this structure allows the antenna to be miniaturized while the bandwidth is increased. The decoupling structure on the ground is made up of three slits and one triangular chamfer.

2. ANTENNA DESCRIPTIONS

2.1. Antenna Structure

The structure and parameters of the antenna are shown in Figure 1. The overall size of the proposed antenna is only $34 \times 34 \text{ mm}^2$. It consists of four orthogonal cup-like radiation elements placed symmetrically inside the gap on the coplanar ground. Three slits and a triangular notch are etched on the ground between two elements. The feedline is integrated on the other side of the substrate and also placed orthogonally at opposite corners of the dielectric substrate. The feedline is connected to the radiation elements through several metal vias cut out in the dielectric substrate. The detailed dimensions of the proposed antenna are optimized by using the commercial software HFSS and shown in Table 1.

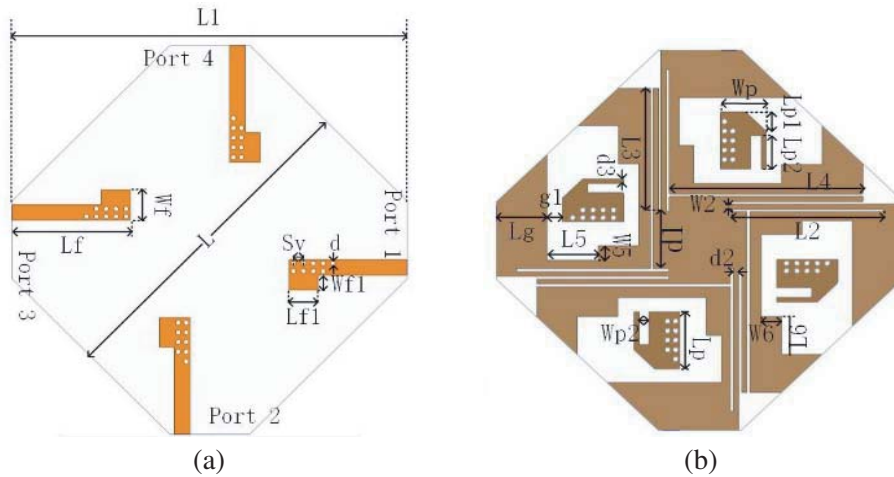


Figure 1. Geometry of the proposed antenna. (a) Top view. (b) Bottom view.

Table 1. Dimensions of the proposed antenna.

Parameters	L	L_1	L_2	L_3	L_4	L_5	L_6	L_f	L_{f1}
Values/mm	34	40	15	13	19	5	4	12	3
Parameters	L_p	L_{p1}	L_{p2}	L_g	W_2	W_5	W_6	W_f	W_{f1}
Values/mm	6	2	3.5	5	0.3	0.5	2	3.1	1.5
Parameters	W_p	W_{p2}	S_v	d	d_1	d_2	d_3	g_1	
Values/mm	4.5	1	1	0.5	6	0.5	0.5	1.5	

2.2. Antenna Isolation Design

In order to achieve the high isolation between antenna elements, a decoupling structure is integrated on the coplanar ground in Figure 2. Three slits are engraved on the ground between each two elements, and one is connected to another group of slits. The decoupling structure functions as a stopband filter, and the degree of coupling changes with the size of the three slits. As shown in Figure 2, when no decoupling structure is added to the ground of the antenna, the isolation of adjacent elements is greater than 15 dB, and the isolation of diagonal elements is greater than 13 dB. When a defective ground structure is loaded on the antenna ground, the isolations of adjacent elements and diagonal elements are improved to 18 dB. The defect ground structure greatly improves the isolation between antenna elements without increasing the complexity of the antenna.

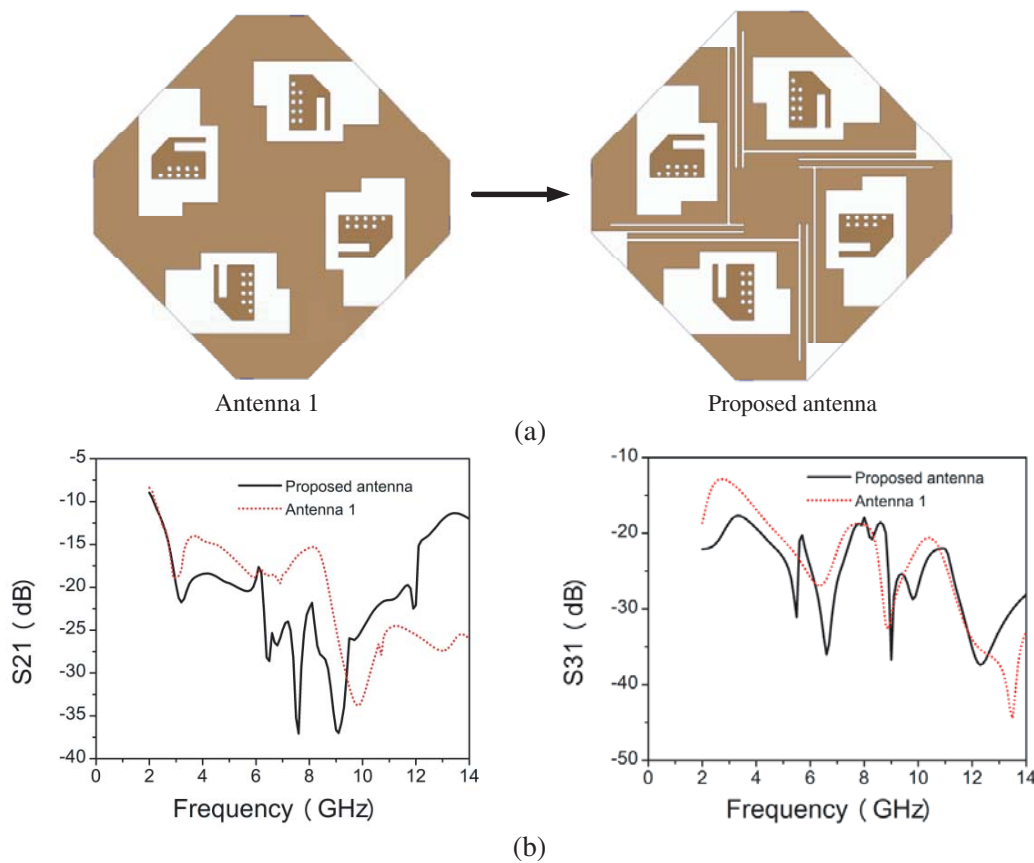


Figure 2. (a) The evolution of the proposed antenna. (b) Simulated S -parameters.

The simulated current distributions of the proposed antenna at 4.5 GHz, 7.5 GHz, and 9.5 GHz are shown in Figure 3. When port 1 is excited, it can be clearly seen that the current is distributed on port 1 of the antenna and the defective ground structure, and almost no current flows on other ports. The surface current distributions validate the decoupling effect of the defective ground structure.

2.3. Antenna Miniaturization Design

In order to achieve miniaturization, it is also necessary to meet the bandwidth requirements of the antenna, so that nine periodically distributed metal vias are integrated into the substrate. The metal vias connect the patches and feedlines at both ends of the substrate, shortening the electrical length of the current path and creating a higher resonant frequency. By changing the position and number of metal holes, the antenna is miniaturized while increasing the bandwidth to meet the requirements of UWB antenna.

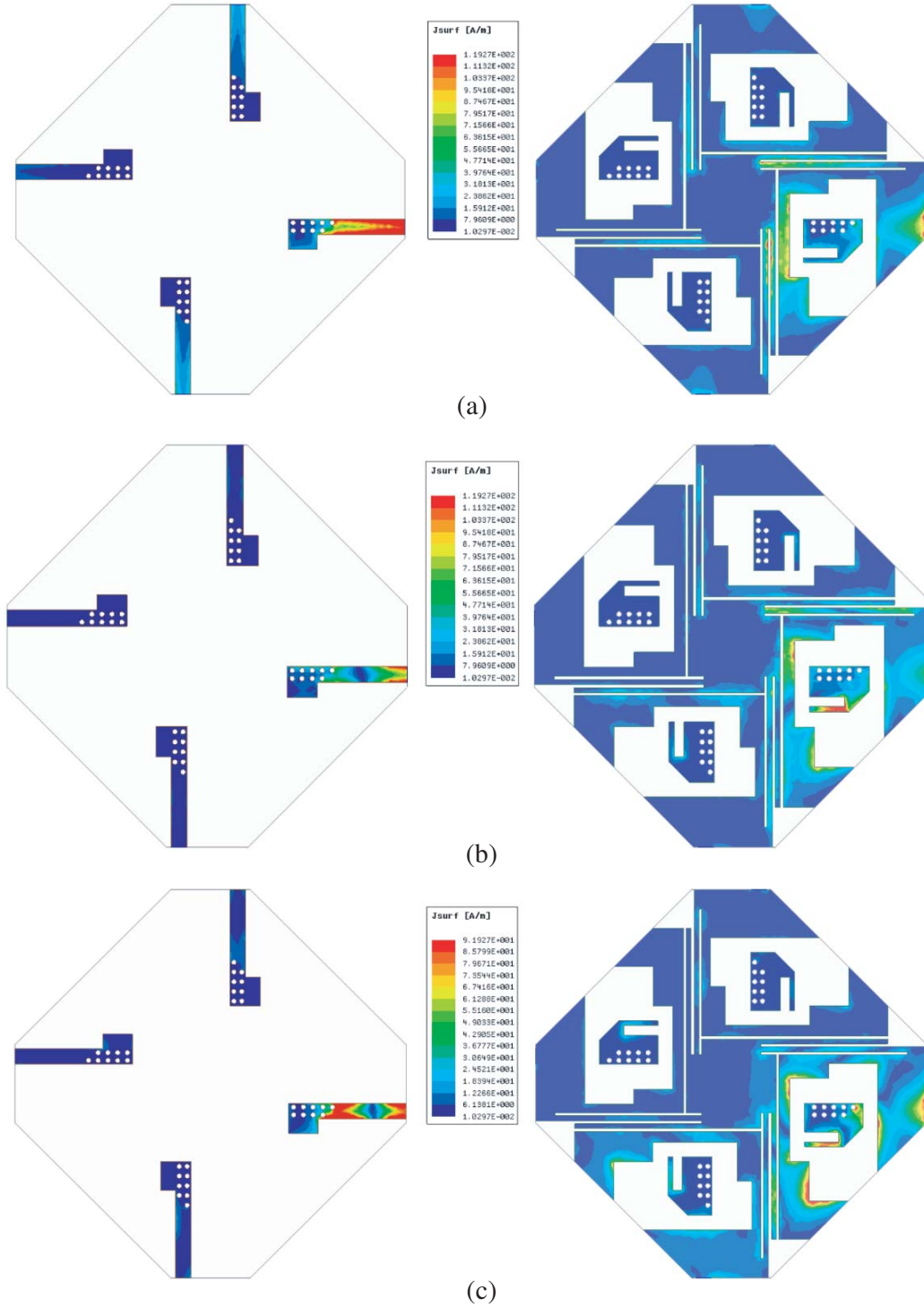
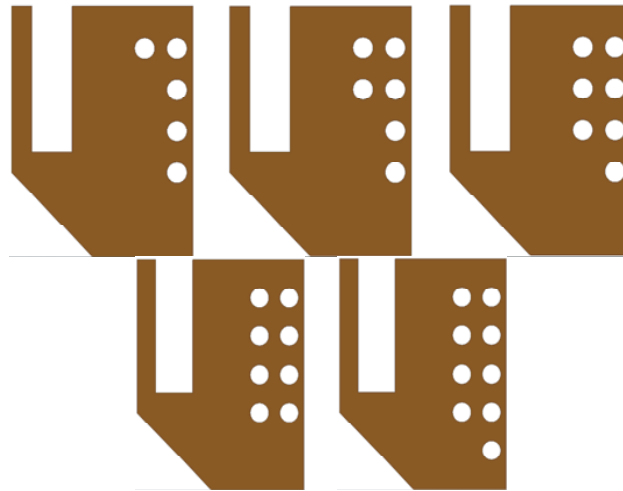
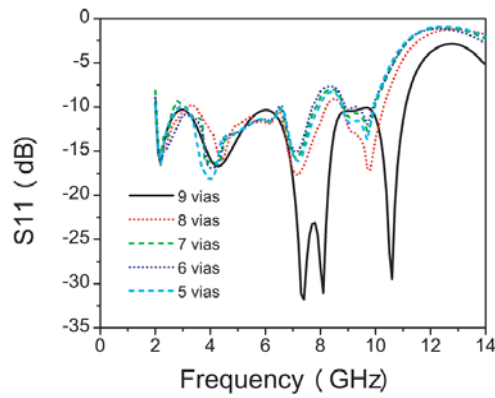


Figure 3. Simulated surface current distributions of the proposed antenna while feeding only port 1. (a) 4.5 GHz. (b) 7.5 GHz. (c) 9.5 GHz.

The effect of the number of metal vias on the antenna bandwidth is studied in this paper. Different numbers of metal vias are excavated in the dielectric substrate between the radiating element and the feedline, and the simulated S_{11} results are shown in Figure 4. When the number of metal vias is 9, the antenna has the best impedance bandwidth at high frequencies, covering the ultra-wideband range.



(a)

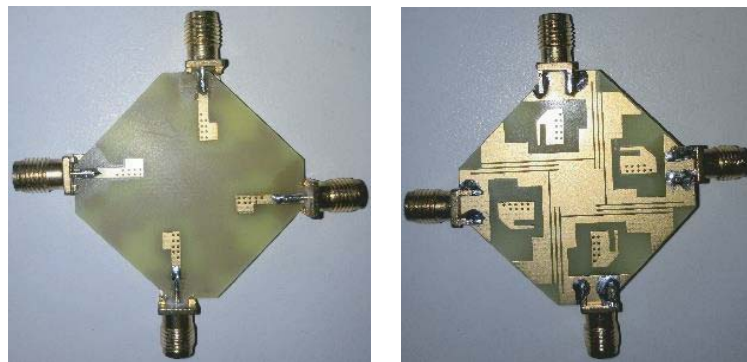


(b)

Figure 4. (a) Changes in the number of metal vias. (b) Simulated S_{11} .

3. RESULTS AND DISCUSSIONS

The proposed MIMO antenna was fabricated on a 1.6 mm FR4 dielectric substrate with relative permittivity of 4.4 and dielectric loss tangent of 0.02, as shown in Figure 5. Since the antenna is



(a)

(b)

Figure 5. Photograph of the fabricated antenna. (a) Top view. (b) Bottom view.

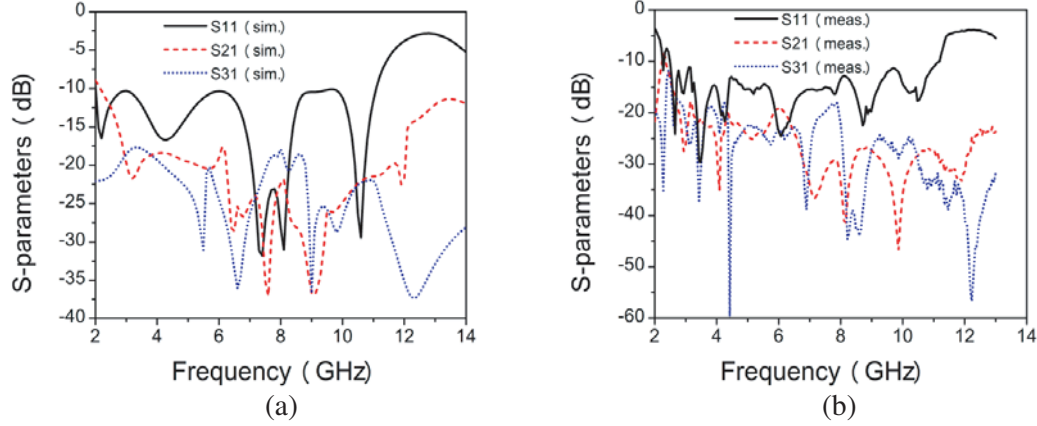


Figure 6. Simulated and measured S -parameters of the proposed antenna. (a) Simulation. (b) Measurement.

symmetrical, the S -parameter between each two ports is equivalent.

Return loss is a key parameter for characterizing the operating bands of the antenna. The simulated and measured results of return loss (S_{11}) are shown in Figure 6. While S_{11} is less than -10 dB, the simulated bandwidth is 2–11 GHz, and the measured bandwidth is 2.5–11.6 GHz. Therefore, the antenna satisfies the impedance matching requirement for the entire UWB specified by the FCC. The measured isolations (S_{21} and S_{31}) are better than 18 dB, which is consistent with the simulated results. According to Figure 6, the simulated results are almost similar to the measured ones, except for some spikes in the measured results, which is due to the loss of the SMA connector during the measurement.

Figure 7 shows the simulation and measurement results of the radiation patterns at 4.5 GHz, 7.5 GHz, and 9.5 GHz. At higher frequencies, due to the design of the decoupling structure on the ground, the current path is changed, and the directionality of the antenna is changed, so that the radiation direction of the antenna has a slight variation. At the lower frequencies, it is observed that the measured results are in agreement with the simulated ones.

The gain is also an important parameter of the antenna for describing the degree of concentration and enlargement of an input power. The measured and simulated results of the peak gain are shown in Figure 8. It can be observed that the gain of the antenna varies from 2 to 6 dBi when frequency changes. In the analysis of the MIMO antenna system, the envelope correlation coefficient (ECC) is a paramount parameter. Figure 8 also shows the simulated ECC values, which are below 0.05 over the entire working frequency band. For a MIMO antenna system, the ECC of less than 0.05 is enough to ensure good channel capacity. In addition, we compare the proposed antenna with other similar works, and the results are listed in Table 2.

Table 2. Comparison with other works.

Reference	No.	Size (mm ²)	Bandwidth (GHz)	Isolation (dB)	Peak Gain (dBi)
[8]	2	18 × 36	2.8–20.0	20	0–4
[9]	2	50 × 30	2.5–14.5	20	1.6–6
[10]	2	25 × 32	3.1–10.6	20	/
[13]	4	50 × 39.8	2.7–12.0	17	2–6
[15]	4	38 × 38	3.0–15.0	20	0–5
[17]	4	40 × 40	3.1–11.0	20	1–4
[18]	2	99.7 × 33.5	2.9–7.1	20	0–6
[19]	4	80 × 80	2.1–20	25	0–5.8
This work	4	34 × 34	2.5–11.6	18	2–6

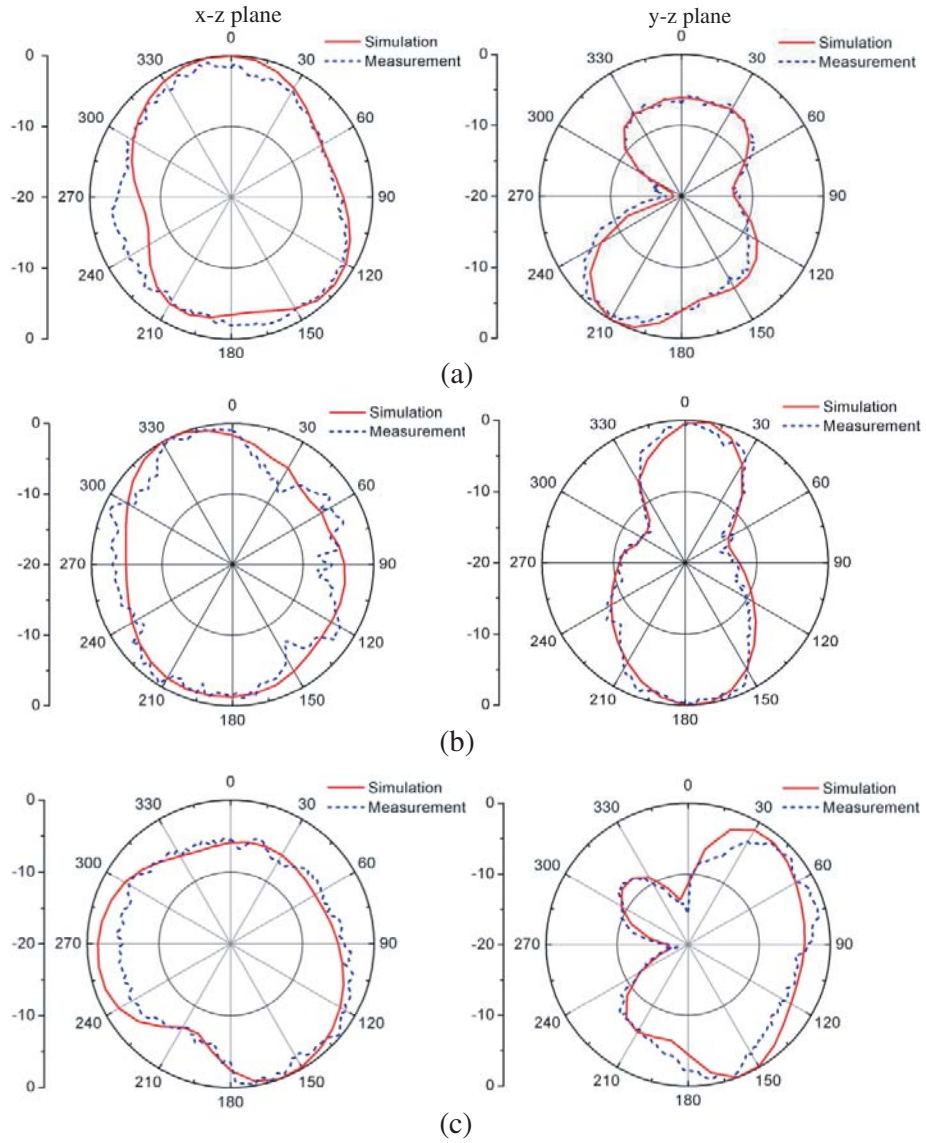


Figure 7. Radiation patterns of the proposed antenna when port 1 is excited. (a) 4.5 GHz. (b) 7.5 GHz. (c) 9.5 GHz.

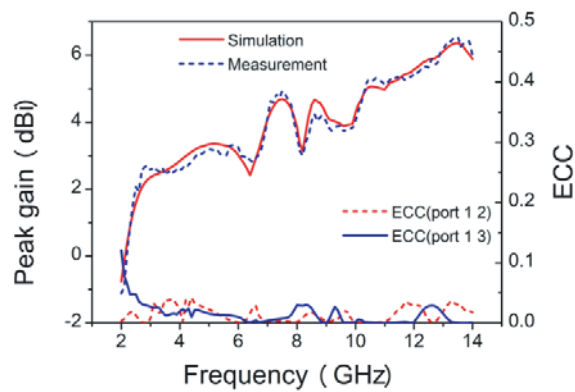


Figure 8. Simulated and measured peak gain and simulated ECC of the proposed antenna.

4. CONCLUSION

A quad-port miniaturized UWB MIMO antenna with metal vias is proposed. The use of metal vias in the antenna increases the bandwidth of the antenna during miniaturizing, and the integration of the decoupling structure on the ground achieves high isolation. Other than that, the miniaturized design of the antenna and the good agreement between the simulation and the measurement results make the proposed antenna a good candidate for short-range communication equipment.

ACKNOWLEDGMENT

This work is supported by the quality engineering project of Anhui Provincial Education Department under Grant 2020kfk335.

REFERENCES

1. Tang, W. and E. Culurciello, "A low-power high-speed ultra-wideband pulse radio transmission system," *IEEE Transactions on Biomedical Circuits and Systems*, Vol. 3, No. 5, 286–292, 2009.
2. Briso, C., C. Calvo, and Y. Xu, "UWB propagation measurements and modelling in large indoor environments," *IEEE Access*, Vol. 7, 41913–41920, 2019.
3. Jiang, W., Y. Cui, B. Liu, W. Hu, and Y. Xi, "A dual-band MIMO antenna with enhanced isolation for 5G smartphone applications," *IEEE Access*, Vol. 7, 112554–112563, 2019.
4. Li, Y., C.-Y.-D. Sim, Y. Luo, and G. Yang, "High-isolation 3.5 GHz eight-antenna MIMO array using balanced open-slot antenna element for 5G smartphones," *IEEE Transactions on Antennas and Propagation*, Vol. 67, No. 6, 3820–3830, 2019.
5. Thummaluru, S. R., R. Kumar, and R. K. Chaudhary, "Isolation and frequency reconfigurable compact MIMO antenna for wireless local area network applications," *IET Microwaves Antennas & Propagation*, Vol. 13, No. 4, 519–525, 2019.
6. Wang, S., Y. Ji, D. Gibbins, and X. Yin, "Impact of dynamic wideband MIMO body channel characteristics on healthcare rehabilitation of walking," *IEEE Antennas and Wireless Propagation Letters*, Vol. 16, 505–508, 2017.
7. Biswas, A. K. and U. Chakraborty, "Compact wearable MIMO antenna with improved port isolation for ultra-wideband applications," *IET Microwaves Antennas & Propagation*, Vol. 13, No. 4, 498–504, 2019.
8. Chandel, R., A. K. Gautam, and K. Rambabu, "Design and packaging of an eye-shaped multiple-input-multiple-output antenna with high isolation for wireless UWB applications," *IEEE Transactions on Components Packaging and Manufacturing Technology*, Vol. 8, No. 4, 635–642, 2018.
9. Iqbal, A., O. A. Saraereh, A. W. Ahmad, and S. Bashir, "Mutual coupling reduction using F-shaped stubs in UWB-MIMO antenna," *IEEE Access*, Vol. 6, 2755–2759, 2018.
10. Ul Haq, M. A. and S. Koziel, "Ground plane alterations for design of high-isolation compact wideband MIMO antenna," *IEEE Access*, Vol. 6, 48978–48983, 2018.
11. Li, W., Y. Hei, P. M. Grubb, X. Shi, and R. T. Chen, "Compact inkjet-printed flexible MIMO antenna for UWB applications," *IEEE Access*, Vol. 6, 50290–50298, 2018.
12. Ghosh, J., S. Ghosal, D. Mitra, and S. R. B. Chaudhuri, "Mutual coupling reduction between closely placed microstrip patch antenna using meander line resonator," *Progress In Electromagnetics Research Letters*, Vol. 59, 115–122, 2016.
13. Khan, M. S., A. D. Capobianco, S. Asif, A. Iftikhar, B. Ijaz, and B. D. Braaten, "Compact 4×4 UWB MIMO antenna with WLAN band rejection operation," *Electronic Letters*, Vol. 51, No. 14, 1048–1055, 2015.
14. Tripathi, S., A. Mohan, and S. Yadav, "A compact koch fractal UWB MIMO antenna with WLAN band-rejection," *IEEE Antennas and Wireless Propagation Letters*, Vol. 14, 1565–1568, 2015.

15. Sipal, D., M. P. Abegaonkar and S. K. Koul, "Easily extendable compact planar UWB MIMO antenna array," *IEEE Antennas and Wireless Propagation Letters*, Vol. 16, 2328–2331, 2017.
16. Wani, Z. and D. Kumar, "A compact 4×4 MIMO antenna for UWB applications," *Microwave and Optical Technology Letters*, Vol. 58, No. 6, 1433–1436, 2016.
17. Ali, W. A. E. and A. A. Ibrahim, "A compact double-sided MIMO antenna with an improved isolation for UWB applications," *AEU-International Journal of Electronics and Communications*, Vol. 82, 7–13, 2017.
18. Ullah, U., I. B. Mabrouk, S. Koziel, et al., "Implementation of spatial/polarization diversity for improved-performance circularly polarized multiple-input-multiple-output ultra-wideband antenna," *IEEE Access*, Vol. 8, 64112–64119, 2020.
19. Rekha, S. D., P. Pardhasaradhi, B. Madha, et al., "Dual band notched orthogonal 4-element MIMO antenna with isolation for UWB applications," *IEEE Access*, Vol. 8, 145871–145880, 2020.
20. Sani, M. M., R. Chowdhury, and R. K. Chaudhary, "An ultra-wideband rectangular dielectric resonator antenna with MIMO configuration," *IEEE Access*, Vol. 8, 139658–139669, 2020.
21. Khan, M. S., A. Iftikhar, R. Shubair, A. D. Capobianco, et al., "Eight-element compact UWB-MIMO/diversity antenna with WLAN band rejection for 3G/4G/5G communications," *Open Journal of Antennas and Propagation*, Vol. 1, 196–206, 2020.